

Experimental Study of K-Band Broadband Antenna Array Using Artificial Inhomogeneous Dielectric Structures

Anton M. Aleksandrin✉, Yury P. Salomatov

Siberian Federal University, Krasnoyarsk, Russia

✉ aalexandrin@sfu-kras.ru

Abstract

Introduction. As a result of the extensive development of broadband communication in the millimetre wave band, there has arisen a need for antenna systems with a high level of directivity and compact dimensions, capable of operating across wide frequency ranges. However, at present, few engineering solutions satisfy this demand.

Aim. To develop and study experimentally a K-band antenna array (AR) characterized by a high aperture efficiency and compact longitudinal dimensions.

Materials and methods. Computer simulations were performed using the CST Studio Suite software. Measurements were carried out using an Agilent E8363B PNA vector circuit analyzer. Radiation patterns were obtained by the method of near-field scanning.

Results. A K-band broadband antenna array configuration operating over the 18...26 GHz range was proposed. It was found that the period of the array equals 2.25 wavelengths at the highest operating frequency. In order to suppress grating lobes, an additional layer consisting of artificial inhomogeneous dielectric lenses was used. The dielectric material consisted of thin curly layers of sheet polyethylene terephthalate. Additionally, a hybrid configuration of feeding network was proposed, in which one part of the network was developed by means of printed two-wire lines, while the other part was achieved by means of rectangular waveguides. The proposed antenna array demonstrates VSWR of less than 2 and an aperture efficiency above 0.5, side and diffractive lobe levels not exceed -12 in the 18...26 GHz range. The total thickness of the configuration equals 50 mm or $4.3\lambda_{\min}$. In order to ensure the compactness of the AR for wideband frequency applications, the thickness of the system can be reduced to $2.5\lambda_{\min}$ by excluding the waveguide part.

Conclusion. When compared with existing solutions, the proposed antenna has a simpler feed network, which yields better matching. High aperture efficiency is achieved in the wide frequency range by means of inhomogeneous dielectric lenses.

Key words: antenna array, broadband antenna, inhomogeneous dielectric, lens antenna

For citation: Aleksandrin A. M., Salomatov Yu. P. Experimental Study of K-Band Broadband Antenna Array Using Artificial Inhomogeneous Dielectric Structures. Journal of the Russian Universities. Radioelectronics. 2019, vol. 22, no. 5, pp. 33–41. doi: 10.32603/1993-8985-2019-22-5-33-41

Conflict of interest. The authors declare no conflict of interest.

Submitted 16.09.2019; accepted 15.10.2019; published online 29.11.2019



Экспериментальное исследование широкополосной антенной решетки К-диапазона с использованием структур из искусственного неоднородного диэлектрика

А. М. Александрин✉, Ю. П. Саломатов

Сибирский федеральный университет, Красноярск, Россия

✉ aalexandrin@sfu-kras.ru

Аннотация

Введение. В связи с освоением миллиметрового диапазона и развитием средств широкополосной связи имеется потребность в антенных системах, которые работали бы в широкой полосе частот (порядка октавной), имели высокую направленность и компактные размеры. Имеющиеся решения, как правило, не удовлетворяют данным требованиям.

Цель работы. Конструирование и экспериментальное исследование антенной решетки (АР) К-диапазона, обладающей высоким коэффициентом использования площади (КИП) и малыми продольными размерами.

Материалы и методы. Численные исследования проводились в САПР СВЧ (CST Studio Suite), экспериментальные исследования – на оборудовании для векторного анализа СВЧ-цепей (Agilent E8363B PNA). Характеристики направленности измерялись методом сканирования ближнего поля.

Результаты. Предложен вариант реализации широкополосной АР К-диапазона (18...26 ГГц). Период АР составляет 2.25 длины волны на верхней частоте диапазона. Для подавления дифракционных лепестков использован дополнительный слой, состоящий из линз из искусственного неоднородного диэлектрика, сформированный из тонких фигурных слоев листового полиэтилентерефталата. Предложена гибридная конфигурация диаграммообразующей схемы (ДОС), в которой одна часть схемы выполнена на основе печатных двухпроводных линий передачи, а другая – на прямоугольных волноводах. АР имеет КСВ ниже 2 и КИП выше 0.5, уровень боковых и дифракционных лепестков не превышает –12 в диапазоне 18...26 ГГц. Суммарная толщина всей системы составила 50 мм, что равно $4.3\lambda_{\min}$. Если из конструкции исключить волноводную часть, толщина может быть уменьшена до $2.5\lambda_{\min}$, что обеспечивает компактность АР при широкой полосе рабочих частот.

Заключение. По сравнению с имеющимися решениями антенна имеет более простую ДОС, за счет чего улучшается согласование с фидером. За счет применения линз из неоднородного диэлектрика обеспечивается высокий апертурный КИП в широкой полосе частот.

Ключевые слова: антенная решетка, широкополосная антенна, неоднородный диэлектрик, линзовая антенна

Для цитирования: Александрин А. М., Саломатов Ю. П. Экспериментальное исследование широкополосной антенной решетки К-диапазона с использованием структур из искусственного неоднородного диэлектрика // Изв. вузов России. Радиоэлектроника. 2019. Т. 22, № 5. С. 33–41. doi: 10.32603/1993-8985-2019-22-5-33-41

Конфликт интересов. Авторы заявляют об отсутствии конфликта интересов.

Статья поступила в редакцию 16.09.2019; принята к публикации после рецензирования 15.10.2019; опубликована онлайн 29.11.2019

Introduction. Currently, the millimetre-wave band is a topic of intensive study due to the need to increase the bandwidth capacity of information transmission channels, develop broadband communications and radar applications [1–3]. Broadband satellite K-band Internet access programmes are under active

development [4]. Moreover, there is a growing need for broadband radio monitoring and radio measurements. In this connection, one of the key determinants of the technical and operational efficiency of such systems is the antennas used.

The widespread use of these systems imposes specific requirements on their antenna systems, which should be broadband, compact, easy to install and deploy, as well as having a low cost. However, the requirements for compactness, bandwidth and high directivity are somewhat contradictory:

- broadband spot beam antennas based on mirrors and lenses have remote elements and, accordingly, significant longitudinal dimensions;
- compact antenna arrays (AAs), produced by printing technology, generally work in a narrow band of frequencies and often have a very complex feeding network (FN), which complicates their coordination across a wide frequency range;
- some types of broadband and compact antennas (e.g., log-periodic) do not provide sufficient directivity to meet the requirements described above.

In order to solve the described problems, the present paper proposes an AA-containing focusing lenses having an artificial inhomogeneous dielectric structure. Lenses narrow the main lobe of the radiation pattern (RP) of the AA element by effectively suppressing the grating lobes, thus allowing operation across a wide frequency range.

The paper [5] presents a method for the realisation of inhomogeneous dielectric lenses (IDLs), defining the limiting values of sampling parameters of the IDL's homogeneous dielectric structure, such as the thickness of the elementary cylindrical layer and the quantity of the figured "lobes" realising the variable law of change of dielectric permittivity [6]. In the paper [7], an AA design with an IDL consisting of 16 elements arranged hexagonally is considered.

In the present article, an AA comprised of 64 elements having a hybrid type FN based on printed two-wire lines and waveguides is considered. This configuration is used to reduce losses in printed lines by replacing some of them with waveguides, in which attenuation is significantly lower.

The AA under development is designed for operation in the K-band (18...26 GHz).

Description of experimental samples. Beam-forming arrangement. In order to avoid grating lobes when the AA is operated over a wide frequency band, the period is set at 0.5 times the wavelength at the upper range limit λ_{\min} . The wavelength determines the dimensions of broadband emitters at the lower operating frequency λ_{\max} . At a specific bandwidth, the emitters inevitably overlap with each other. Broadband AAs are known to use the emitter configuration based on overcoupled vibrators. In such AAs, the ends

of vibrators overlap each other, forming an interdigitated pattern [8]. There are different variations of such AAs with different ways of "packing" the emitters on the plane, for example, intertwined spirals [9].

Besides overcoupled vibrators, there are also AAs based on long slots [10–12].

The drawbacks of these methods are as follows:

- it is impossible to place the FN on a common substrate with emitting elements. This results in the need to provide transition elements between transmission lines of different types, which, in turn, complicates the coordination;
- the density of emitters is very high, since the period of the structure must be shorter than $0.5\lambda_{\min}$. This leads to difficulties in the FN design for such a grating and a deterioration in coordination.

Another approach to extending the effective AA bandwidth is to increase its period by reducing the number of elements and thus simplifying the FN. In this case, it is necessary to use focusing elements narrowing the RP of each emitter in order to suppress the grating lobes. Lenses having an inhomogeneous dielectric structure can be used for these elements [13–15].

In the considered design, the emitters are printed broadband "bowtie" vibrators etched on a substrate of Rogers RT5880 material with an angle of dielectric loss tangent $\text{tg}\delta=0.0009$, which corresponds to losses of 4 dB/m at a frequency of 26 GHz (Fig. 1).

The vibrator arms are located on different sides of the substrate and are powered by a printed two-wire line (TWL) supplied to the center of the vibrator. The elements are located hexagonally; the FN has a binary-floor configuration. The AA period is 26 GHz 3.25λ at the upper frequency.

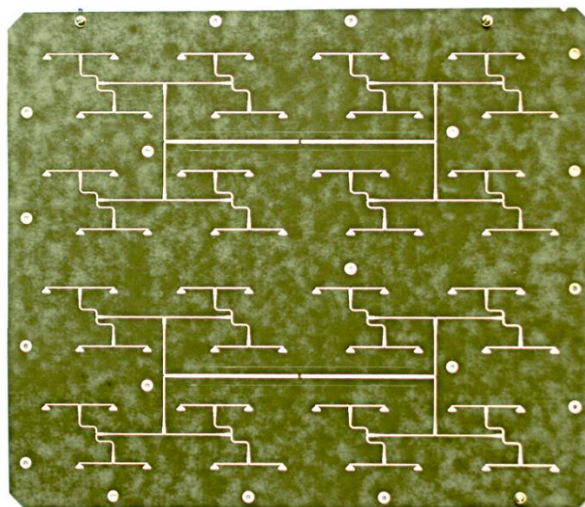


Fig. 1. Feeding network circuit

The first two stages of the divider are made based on a waveguide line of the WR42 standard, which has a size of 10.67×4.32 mm and an attenuation rate of 0.4 dB/m. A waveguide is formed by two aluminium parts. The first part forms one of the wide walls of the waveguide, as well as serving as a reflective screen for the AA elements and the bearing element for the lens attachment (Figs. 2, 1), while the second part in the form of a rectangular groove in a thick plate forms the remaining three walls of the waveguide (Figs. 2, 2 and 3). A special smooth transition is used to interface the printing line with the waveguide.

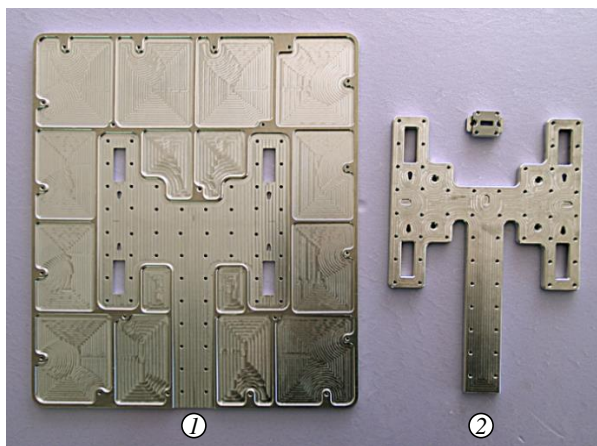


Fig. 2. Waveguide divider (without transitions to two-wire line)

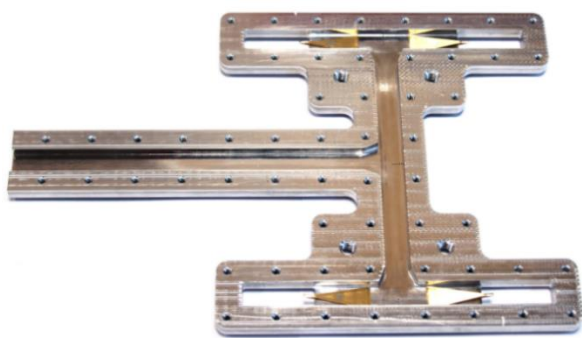


Fig. 3. Bottom part of the waveguide divider (inside view). Lines end with transitions to two-wire line

Two-wire waveguide transition. Fig. 4 presents the isometric transition from the rectangular waveguide to the printed two-wire line. The two-wire waveguide transition consists of a smooth linear transition of the rectangular waveguide to the ridged waveguide with a subsequent smooth transition to a printed line. The dielectric substrate of the printing line enters the space between the ridges of the ridged waveguide and ends with a triangular dielectric contraction. Line conductors terminate at the place of transition to the waveguide ridges.

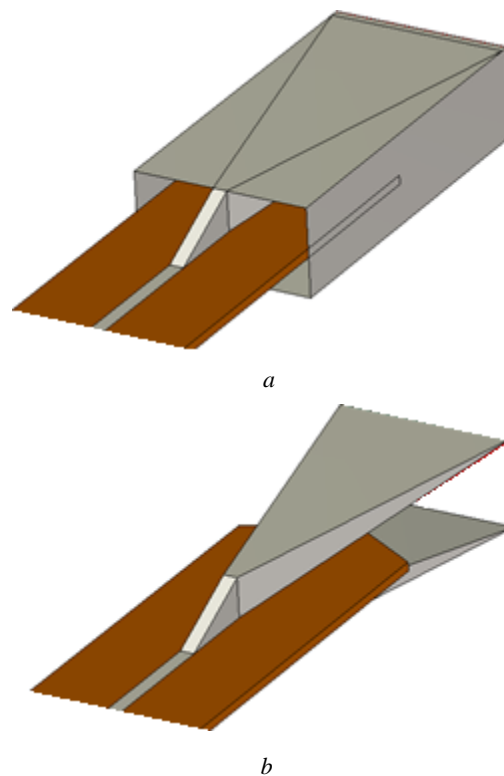


Fig. 4. Isometric view from the waveguide to transition two-wire symmetrical line:
 a – completely; b – without the walls of the waveguide

The experimental study measured the reflection coefficient (RC) of the system of two identical transitions connected by a 140 mm TWL segment (Fig. 5).

The described system has two waveguide ports, reflecting both the input and output ports. Frequency response filtering S_{11} is applied in the temporary area to eliminate the effect of reflections from the output port. This feature is provided by an Agilent E8363B PNA.

Figs. 6, 7 show a possible way to connect a printed TWL to a waveguide by means of this transition. In this case, a flexible substrate is used, in which a "reed" is cut out between the two ridges of the ridged waveguide.



Fig. 5. Experimental circuit from two transitions connected with a fragment of the two-wire line

Experimental AA model. The full AA model (Fig. 8) consists of 64 emitters located in the nodes of the hexagonal grid.

The upper wall of the rectangular waveguide is the lower part of the metal plate, which also acts as a screen (Fig. 2). The other three walls are formed by rectangular grooves in the counterpart of the waveguide divider.

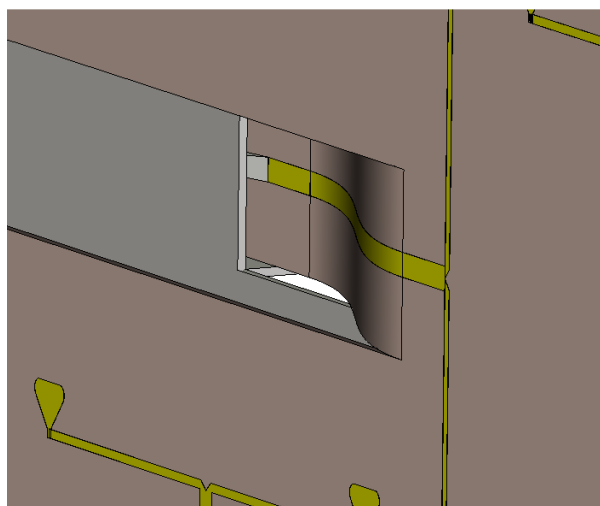


Fig. 6. Front view of the transition from the waveguide to two-wire line

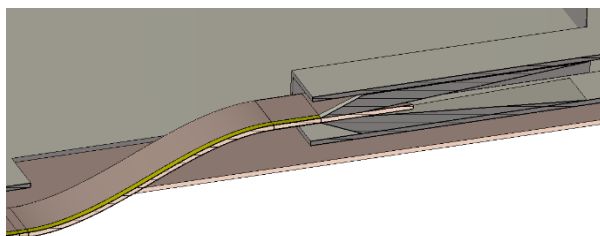


Fig. 7. Inside construction of the transition, cross-section through E -plane of the waveguide

The focusing layer is made up of 22 layers of 1-mm-thick sheet polyethylene terephthalate (PET), from which the lobes are laser cut to create lenses.

Between the screen, the FN board and the lens layer, there are gaps of 5.2 and 2 mm, respectively, which are provided with foam polystyrene layers, as well as plastic washers of appropriate thickness. All structure layers are screwed together around the perimeter and at 5 central points.

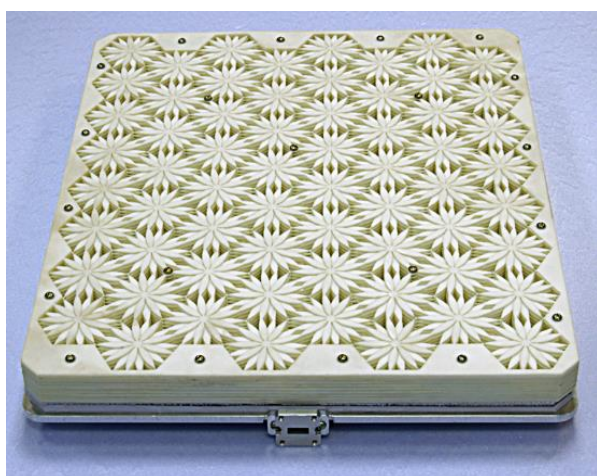


Fig. 8. Experimental model of the antenna array (top view)

The AA model dimensions are $330 \times 290 \times 50$ mm, therefore, the longitudinal size of the antenna is $4.3\lambda_{\min}$.

Research methods. The emitting structures were simulated numerically using CST Studio Suite. The characteristics of the experimental sample of the waveguide-two-wire transition were measured by the Agilent E8363B PNA vector circuit analyser, which allows the S -parameters of the four poles to be measured in the frequency band of 0.01...40 GHz. This device also provides filtration of the obtained characteristics in the time domain, allowing the influence of reflections from certain elements of the measured circuit to be excluded. In order to measure the directional characteristics, a hardware and software complex developed at the Radio Engineering Department of the Siberian Federal University was used to measure the characteristics of antennas in the near zone. This apparatus consists of an anechoic chamber, a four-axis flat scanner and software for processing measurements. The RP and the directivity were calculated from the amplitude and phase distribution in the antenna array. The gain was measured using the reference antenna method.

Research results. Waveguide-two-wire transition. Fig. 9 shows the frequency characteristics of the RC module for several transition lengths (L_{tr}).

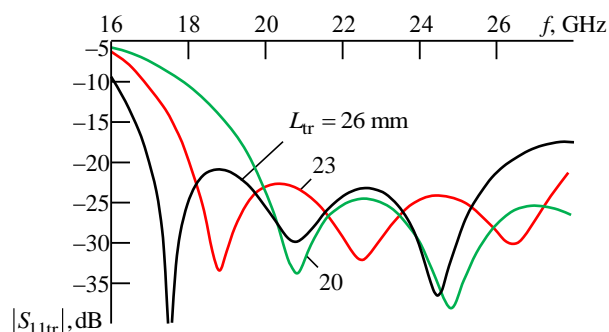


Fig. 9. Simulated frequency dependences of the reflection coefficient modulus of the waveguide two-wire transition

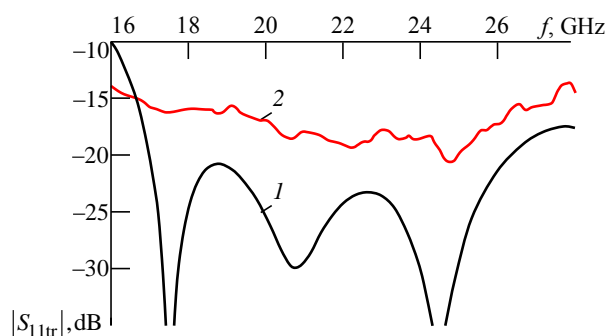


Fig. 10. Reflection coefficient of the transition from waveguide to two-wire line:
 1 – calculation for $L_{tr} = 26$ mm; 2 – experiment

Following the calculation data, the experimental transition length was selected equal to 26 mm, which corresponds to its work in the range of 18...26 GHz.

Fig. 10 shows the frequency dependence S_{11tr} , obtained by excluding reflections from the second port by filtering in the time domain. The calculated curve corresponds to a transition length of 26 mm.

Experimental AA model. In the course of experimental studies of the AA model, the RC (Fig. 11), RP at the upper frequency of the working range in the sections $\varphi = 0, 30, 60$ and 90° (Fig. 12), side lobes levels (SLL) in these RP sections and frequency dependencies of the directivity and gain were measured.

Fig. 13 shows diagrams of the SLL in different sections of the three-dimensional characteristic of the AA directivity. SLL here means the highest level of any of the side lobes of the antenna. In the E ($\varphi = 90^\circ$) and

H ($\varphi = 0$) planes, this was the first side lobe, the level of which was approximately -12 dB across the entire frequency band.

Fig. 14 shows the experimental frequency dependencies of the directivity antenna (D_{exp}), gain (G_{exp}); the directivity graph of the co-phased uniformly excited ideal aperture (D_{id}), of the equal studied antenna area is presented for comparison.

Discussion. Two-wire waveguide transition. The essential dimensional parameter of the transition is its length (L_{tr}). Numerical studies show that this parameter determines the lower operating frequency of the transition. The overlap ratio of the working transition band at -20 dB is approximately 1.5. As can be seen from Fig. 10, the transfer ratio of the experimental waveguide-two-wire transition in the working

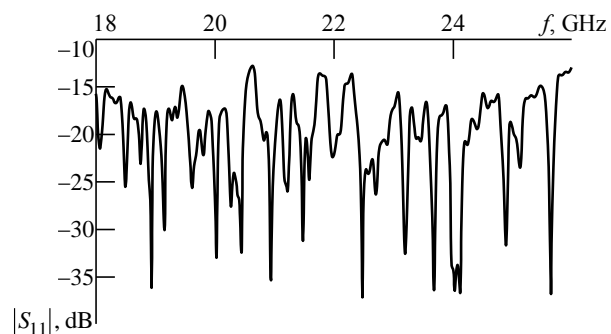


Fig. 11. Reflection coefficient from the antenna input

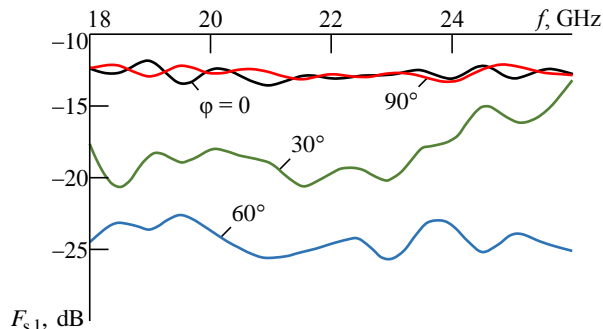


Fig. 13. The level of the maximum side lobe of the antenna radiation pattern

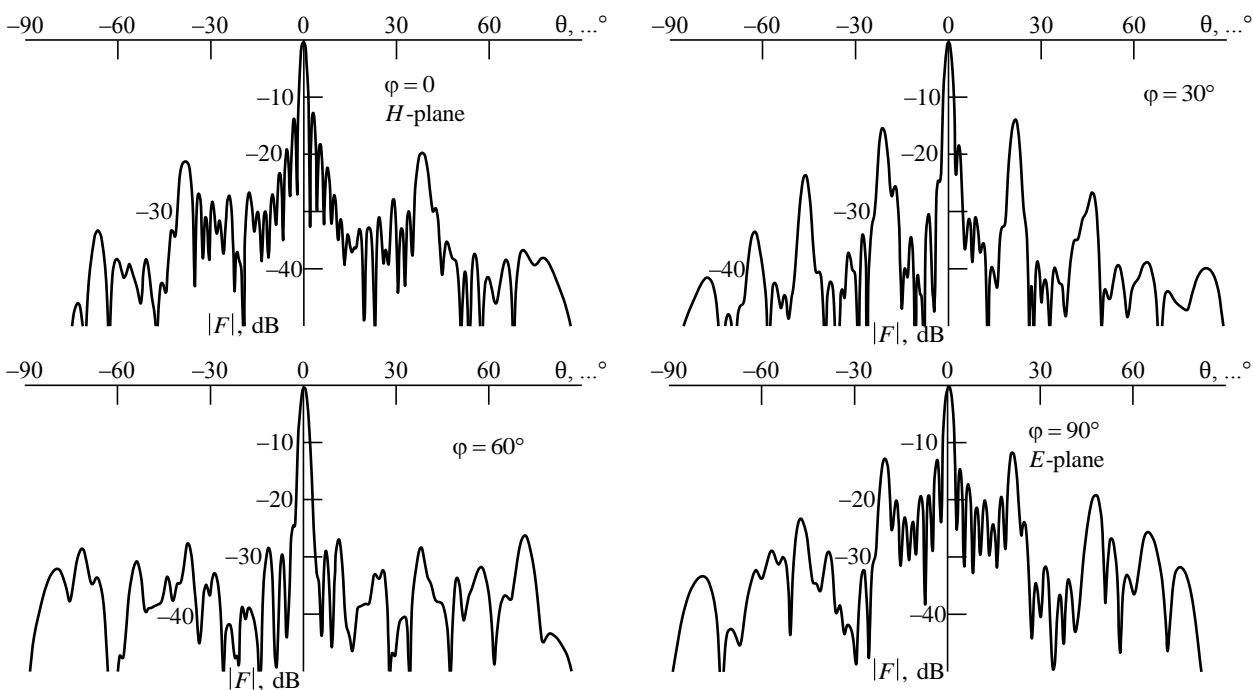


Fig. 12. Array radiation pattern at the frequency 26 GHz

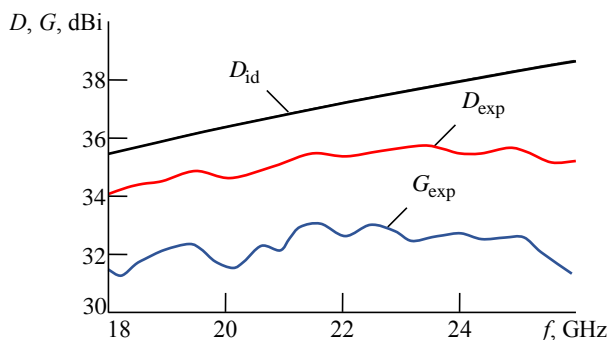


Fig. 14. Experimental dependencies of the directivity (D_{exp}) and gain (G_{exp}) of the antenna, the directivity of an ideal aperture (D_{id})

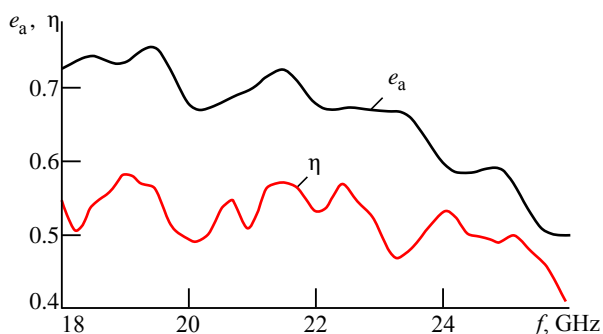


Fig. 15. Aperture efficiency (e_a) and energy efficiency of the antenna (η)

frequency band does not exceed -15 dB, but is significantly higher than the calculated data. This discrepancy may be due to the inaccuracy in the positioning of the printed line conductors relative to the waveguide ridges and the insufficiently precise selection of the width of the two-wire line, which results in a mismatch.

AA model. Since the aperture efficiency (AE) of a single emitter is less than 1, the grating lobes in the AA are not entirely suppressed. However, in the frequency band of 18...26 GHz, their level does not exceed the level of the first side lobe, which is -12 dB. It follows from the experimental data that the grating period $3.25\lambda_{\text{min}}$, is too long for the grating lobe level criterion: at the upper frequency, their level reaches -12 dB. The grating lobes can be slightly reduced by shortening the grating period.

The AE (e_a) of the antenna is in the working frequency band above 0.5 (Fig. 15). The efficiency (η) of the experimental sample is approximately 0.5, dropping to 0.25 at the upper band limit. The AE can be increased by reducing the grating period, while the use of lower loss materials is required to increase efficiency.

Conclusion. The AA considered in the article allows the standard IEEE-band of 18...26 GHz to be covered; the AE in the frequency band exceeds 0.5, while the level of side and the grating lobes do not exceed -12 dB. The application of a hybrid FN based on printed two-wire and waveguide lines allows losses in the printed line to be reduced. Although the overall efficiency of the experimental layout was relatively low, this can be corrected by the use of lower loss dielectrics for lens fabrication (e.g., polystyrene).

The total thickness of the whole system was 50 mm, which is equivalent $4.3\lambda_{\text{min}}$. If the waveguide part is excluded from the design, the thickness can be reduced to $2.5\lambda_{\text{min}}$ to ensure compactness of the AA at a wide working frequency range.

References

1. Pi Z., Khan F. An Introduction to Millimeter-Wave Mobile Broadband Systems. IEEE Communications Magazine. 2011, vol. 49, iss. 6, pp. 101–107. doi: 10.1109/MCOM.2011.5783993
2. Cudak M., Ghosh A., Kovarik T., Ratasuk R., Thomas T. A., Vook F. W., Moorut P. Moving Towards Mmwave-Based Beyond-4G (B-4G) Technology. 2013 IEEE 77th Vehicular Technology Conf. Dresden, Germany, 2–5 June 2013. Piscataway, IEEE, 2013, pp. 1–5. doi: 10.1109/VTCSpring.2013.6692638
3. Shaddadab R. Q., Mohammada A. B., Al-Gailaniac S. A., Al-hetarb A. M., Elmagzouba M. A. A Survey on Access Technologies for Broadband Optical and Wireless Networks. J. of Network and Computer Applications. 2014, vol. 41, pp. 459–472. doi: 10.1016/j.jnca.2014.01.004
4. Selva D., Golkar A., Korobova O., Lluch i Cruz I., Collopy P., de Weck O. L. Distributed Earth Satellite Systems: What is Needed to Move Forward? J. of Aerospace Information Systems. 2017, vol. 14, no. 8, pp. 412–438. doi: 10.2514/1.1010497
5. Alexandrin A. M. Implementation of a Radially Inhomogeneous Medium and Construction of the Aperture Antennas on its Basis. 2013 Intern. Siberian Conf. on Control and Communications (SIBCON 2013). Krasnoyarsk, Russia, 12–13 Sept. 2013. Piscataway, IEEE, 2013. doi: 10.1109/SIBCON.2013.6693593
6. Alexandrin A. M., Ryazantsev R. O., Salomatov Y. P. Numerical Optimization of the Discrete Mikaelian Lens. 2016 Intern. Siberian Conf. on Control and Communications (SIBCON 2016). Moscow, Russia, 12–14 May 2016. Piscataway, IEEE, 2016. doi: 10.1109/SIBCON.2016.7491859
7. Aleksandrin A. M., Salomatov Yu. P. Wideband Antenna Array with the Use of Artificial Inhomogeneous Dielectric Structures. Doklady Tomskogo gosudarstvennogo

universiteta sistem upravleniya i radioelektroniki [Proc. of Tomsk State University of Control Systems and Radioelectronics]. 2012, no. 2 (26), pp. 7–10. (In Russ.)

8. Munk B. A. *Finite Antenna Arrays and FSS*. Hoboken, NJ, USA: John Wiley & Sons, Inc, 2003, 392 p.

9. Gross F. B. *Frontiers in Antennas: Next Generation Design & Engineering*. New York, McGraw-Hill, 2011, 526 p.

10. Volakis J. L. *Antenna Engineering Handbook*. New York, McGraw-Hill, 2007, 1754 p. doi: 10.1002/9780471730071.ch1

11. Lee J. J., Livingston S., Nagata D. A Low Profile 10:1 (200–2000 MHz) Wide Band Long Slot Array. 2008 IEEE Antennas and Propagation Society Intern. Symp. San Diego, CA, USA, 5–11 July 2008. Piscataway, IEEE, 2008, vol. 1, pp. 61–64. doi: 10.1109/APS.2008.4619302

12. Youn H. S., Lee Y. L., Celik N., Iskander M. F. Design of a Cylindrical Long-Slot Array Antenna Integrated with

Hybrid EBG/Ferrite Ground Plane. *IEEE Antennas Wireless Propagation Lett.* 2012, vol. 11, pp. 180–183. doi: 10.1109/LAWP.2012.2186782

13. Yi J., de Lustrac A., Piau G.-P., Burokur S. N. Lenses Designed by Transformation Electromagnetics and Fabricated by 3D Dielectric Printing. 2016 IEEE Antennas Propag. Soc. Int. Symp. (APSURSI 2016). Fajardo, Puerto Rico, 26 June–1 July 2016. Piscataway, IEEE, 2016, pp. 1385–1386. doi: 10.1109/APS.2016.7696399

14. Kotljar V. V., Meljohin A. S. Abel Transform in Synthesis of Gradient Optical Elements. *Computer Optics.* 2002, no. 3, pp. 29–36. (In Russ.)

15. Triandafilov Ya. R., Kotlyar V. V. Photonic Crystal Mikaelian Lens. *Computer Optics.* 2007, vol. 31, no. 3, pp. 27–31. (In Russ.)

Information about the authors

Anton M. Aleksandrin, Master's degree in Radio Engineering (2009), postgraduate, senior lecturer of Radio Engineering Department of the Siberian Federal University (SFU). The author of 20 scientific publications. Area of expertise: antennas and microwave devices; wideband antennas and antenna arrays.

Address: Siberian Federal University, 79 Svobodny Str., Krasnoyarsk 660041, Russia

E-mail: aalexandrin@sfu-kras.ru

<https://orcid.org/0000-0002-8428-5562>

Yury P. Salomatov, Cand. Sci. (Eng.) (1982), Professor (2013) of Department of Radio Engineering of the Siberian Federal University. The author of 240 scientific publications. Area of expertise: phased arrays; digital phased arrays; quasi-optical antennas and antenna arrays.

Address: Siberian Federal University, 79 Svobodny Str., Krasnoyarsk 660041, Russia

E-mail: ysalomatov@sfu-kras.ru

<https://orcid.org/0000-0003-4309-226X>

Список литературы

1. Pi Z., Khan F. An Introduction to Millimeter-Wave Mobile Broadband Systems // IEEE Communications Magazine. 2011. Vol. 49, iss. 6. P. 101–107. doi: 10.1109/MCOM.2011.5783993
2. Moving Towards Mmwave-Based Beyond-4G (B-4G) Technology / M. Cudak, A. Ghosh, T. Kovarik, R. Ratasuk, T. A. Thomas, F. W. Vook, P. Moorut // 2013 IEEE 77th Vehicular Technology Conf. Dresden, Germany, 2–5 June 2013. Piscataway: IEEE, 2013. P. 1–5. doi: 10.1109/VTCSpring.2013.6692638
3. A Survey on Access Technologies for Broadband Optical and Wireless Networks / R. Q. Shaddadab, A. B. Mohammeda, S. A. Al-Gailaniac, A. M. Al-hetarb, M. A. Elmagzouba // J. of Network and Computer Applications. 2014. Vol. 41. P. 459–472. doi: 10.1016/j.jnca.2014.01.004
4. Distributed Earth Satellite Systems: What is Needed to Move Forward? / D. Selva, A. Golkar, O. Korobova, I. Lluch i Cruz, P. Collopy, O. L. de Weck // J. of Aerospace Information Systems. 2017. Vol. 14, № 8. P. 412–438. doi: 10.2514/1.1010497
5. Alexandrin A. M. Implementation of a Radially Inhomogeneous Medium and Construction of the Aperture Antennas on its Basis // 2013 Intern. Siberian Conf. on Control and Communications (SIBCON 2013). Krasnoyarsk, Russia, 12–13 Sept. 2013. Piscataway: IEEE, 2013. doi: 10.1109/SIBCON.2013.6693593
6. Alexandrin A. M., Ryazantsev R. O., Salomatov Yu. P. Numerical Optimization of the Discrete Mikaelian Lens // 2016 Intern. Siberian Conf. on Control and Communications (SIBCON 2016). Moscow, Russia, 12–14 May 2016. Piscataway: IEEE, 2016. doi: 10.1109/SIBCON.2016.7491859
7. Александрин А. М., Саломатов Ю. П. Широкополосная антенная решетка с использованием структур из искусственного неоднородного диэлектрика // Докл. Томского государственного университета систем управления и радиоэлектроники. 2012. № 2 (26). С. 7–10.
8. Munk B. A. Finite Antenna Arrays and FSS. Hoboken, NJ, USA: John Wiley & Sons, Inc, 2003. 392 p.
9. Gross F. B. Frontiers in Antennas: Next Generation Design & Engineering. New York: McGraw-Hill, 2011. 526 p.
10. Volakis J. L. Antenna Engineering Handbook. New York: McGraw-Hill, 2007. 1754 p. doi: 10.1002/9780471730071.ch1
11. Lee J. J., Livingston S., Nagata D. A Low Profile 10:1 (200–2000 MHz) Wide Band Long Slot Array // 2008 IEEE Antennas and Propagation Society Intern. Symp. San Diego, CA, USA, 5–11 July 2008. Piscataway: IEEE, 2008. Vol. 1. P. 61–64. doi: 10.1109/APS.2008.4619302
12. Design of a Cylindrical Long-Slot Array Antenna Integrated with Hybrid EBG/Ferrite Ground Plane / H. S. Youn, Y. L. Lee, N. Celik, M. F. Iskander // IEEE Antennas Wireless Propagation Lett. 2012. Vol. 11. P. 180–183. doi: 10.1109/LAWP.2012.2186782
13. Lenses Designed by Transformation Electromagnetics and Fabricated by 3D Dielectric Printing / J. Yi, A. de Lustrac, G.-P. Piau, S. N. Burokur // 2016 IEEE Antennas Propag. Soc. Int. Symp. (APSURSI 2016). Fajardo, Puerto Rico, 26 June–1 July 2016. Piscataway: IEEE, 2016. P. 1385–1386. doi: 10.1109/APS.2016.7696399
14. Котляр В. В., Мелехин А. С. Преобразование Абеля в задачах синтеза градиентных оптических элементов // Компьютерная оптика. 2002. № 3. С. 29–36.
15. Триандафилов Я. Р., Котляр В. В. Фотонно-кристаллическая линза Микаэляна // Компьютерная оптика. 2007. Т. 31, № 3. С. 27–31.

Информация об авторах

Александрин Антон Михайлович – магистр по направлению "Радиотехника" (2009), аспирант, старший преподаватель кафедры "Радиотехника" Сибирского федерального университета. Автор 20 научных работ. Сфера научных интересов – антенны и СВЧ-устройства; широкополосные антенны и антенные решетки. Адрес: Сибирский федеральный университет, пр. Свободный, 79, г. Красноярск, 660041, Россия
E-mail: aalexandrin@sfu-kras.ru
<https://orcid.org/0000-0002-8428-5562>

Саломатов Юрий Петрович – кандидат технических наук (1982), профессор (2013) кафедры "Радиотехника" Сибирского федерального университета. Автор 240 научных работ. Сфера научных интересов – ФАР; ЦФАР; квазиоптические антенны и антенные решетки. Адрес: Сибирский федеральный университет, пр. Свободный, 79, г. Красноярск, 660041, Россия
E-mail: ysalomatov@sfu-kras.ru
<https://orcid.org/0000-0003-4309-226X>